Proc. Nat. Acad. Sci. USA
Vol. 71, No. 12, pp. 4797–4801, December 1974

Focal Erythrocyte Membrane Perturbations Caused by Nitroxide Lipid Analogues

(scanning electron microscopy/osmotic fragility/echinocytes/membrane domains/paramagnetic probes)

V. G. BIERI, D. F. H. WALLACH, AND P. S. LIN

Division of Radiobiology, Department of Therapeutic Radiology, Tufts-New England Medical Center, 136 Harrison Avenue, Boston, Massachusetts 02111

Communicated by J. L. Oncley, September 23, 1974

ABSTRACT **Three classes of lipoidal nitroxide spin probes reversibly perturb erythrocyte membranes at low concentrations (10^{-10}–10^{-5} M). This is manifest in (*a*) decreased osmotic fragility and (*b*) alterations of surface topology. At bulk phase nitroxide concentrations providing maximal osmotic stabilization, the erythrocytes exhibit a classic echinocyte morphology. At nitroxide concentrations very slightly higher than those yielding minimal osmotic fragility (10^{-5}–10^{-4} M), the cells undergo a sphering reaction and lyse. The morphologic sequence seen in intact cells is not observed in erythrocyte ghosts. We suggest that the spin probes initially concentrate in focal domains, which expand into echinocytic protrusions primarily due to localized weakening of membrane cohesion. We propose that cell lysis involves an irreversible breakdown in membrane domain structure.**

Experimentation on model membrane systems indicates that nitroxide labeled lipids might perturb biomembranes (1, 2). For example, spin-labeled cholesterol analogues, spread as monolayers at air-water interfaces occupy markedly greater areas per molecule than that of cholesterol (3). Similarly, at low surface pressures, monolayers of 12-nitroxide stearate form expanded films in which, the spin-labeled fatty acid lies parallel to the air-water interface, with the carboxyl and nitroxide residues anchored in water (4).

Such data lead one to expect that lipid spin probes might locally "fluidize" a lipid environment and recent model studies show that this is so. Thus, various lipid spin probes tumble freely in lipid multilayers at temperatures where the bulk lipid is solid (5).

To what extent can lipoidal nitroxide spin probes perturb biomembranes? We have approached this question for the erythrocyte membrane by means of scanning electron microscopy and Seeman's technique (6, 7). The latter exploits the fact that many membrane-active agents at low concentrations stabilize erythrocytes against osmotic lysis, but, at high concentrations engender membrane disruption.

EXPERIMENTAL

Erythrocytes, always drawn from the same donor, were used within 2 hr. The heparinized venous blood was centrifuged at $1.5 \times 10^4\ g \times$ min, the plasma and leukocytes removed with care, the erythrocytes washed four times with 0.15 M NaCl, 0.01 M phosphate, pH 7.2 and suspended in this medium at a concentration of 10^9 cells per ml. Hemoglobin-free erythrocyte ghosts were prepared as in (8).

2-(3-carboxypropyl)-4,4-dimethyl-2-tridecyl-3-oxazolidinyloxyl (5NS), 2-(14-carboxytetradecyl)-2-ethyl-4,4-dimethyl-3-oxazolidinyloxyl (16NS), and 17β-hydroxy-4'4'-dimethylspiro[5α-androstan-3,2'-oxazolidin]-3'-yloxyl (ASL) were purchased from Syva Comp., Palo Alto, Calif.; 4-(*N*-carbamidoheptadecyl)-2,2,6,6-tetramethyl-*N*-oxylpiperidine (SAMSL) was generously provided by Dr. Ian C. P. Smith (Div. Biological Sci., National Res. Council of Canada, Ottawa). Stock solutions (10^{-4} M) of the spin labels were prepared by diluting 10^{-2} M methanolic solutions with either 0.15 M NaCl, 0.01 M phosphate, pH 7.2, for scanning electron microscopy or 0.065 M NaCl, 0.01 M phosphate, pH 7.2 for the hemolysis tests. Dilutions were carried down to 10^{-10} M, with the same buffers while maintaining the methanol concentration at 1%.

For scanning electron microscopy, the erythrocytes and erythrocyte ghosts were diluted to 10^7 cells in 3 ml of 0.15 M NaCl, 0.01 M phosphate at pH 7.2, 1% methanol, that contained 10^{-4}–10^{-10} M of the spin probe. After 5 min at room temperature the cells were fixed by adding 7.0 ml of 2% glutaraldehyde in Millonig's buffer at pH 7.3 (9), washed twice with deionized water, and then spread on chemically clean glass slides.

Spread cells were air dried at room temperature, shadowed with gold:palladium (60:40), and viewed at 1000× to 10,000× magnification with a JEOLCO model JSM U3 scanning electron microscope operated at 25 kV and 0° tilt angle. Ghost were handled identically but viewed at 45°. For differential counts, seven fields were selected at random and photographed at a magnification of 1 to 3×10^3. Cells incubated for 5 min in buffered saline ±1% methanol were used as controls.

For the hemolysis experiments we incubated 10^7 erythrocytes in 3.0 ml of 0.065 M NaCl, 0.01 M phosphate at pH 7.2, 1% methanol that contained 10^{-4}–10^{-10} M nitroxide. After 5 min at room temperature, unlysed cells were spun down (10^4 rpm for 2 min; Beckman Microfuge) and the absorbance of the supernatant fluid determined at 543 nm in a Gilford 2400 spectrophotometer. Under our conditions 100% hemolysis in 0.01 M phosphate at pH 7.2 yielded an absorbance of

Abbreviations: 5NS, 2-(3-carboxypropyl)-4,4-dimethyl-2-tridecyl-3-oxazolidinyloxy; 16NS, 2-(14-carboxytetradecyl)-2-ethyl-4,4-dimethyl-3-oxazolidinyloxyl; ASL, 17β-hydroxy-4',4'-dimethylspiro [5α-androstan-3,2'-oxazolidin]-3'-yloxyl; SAMSL, 4-(*N*-carbamidoheptadecyl)-2,2,6,6-tetramethyl-*N*-oxylpiperidine; ESR, electron spin resonance.

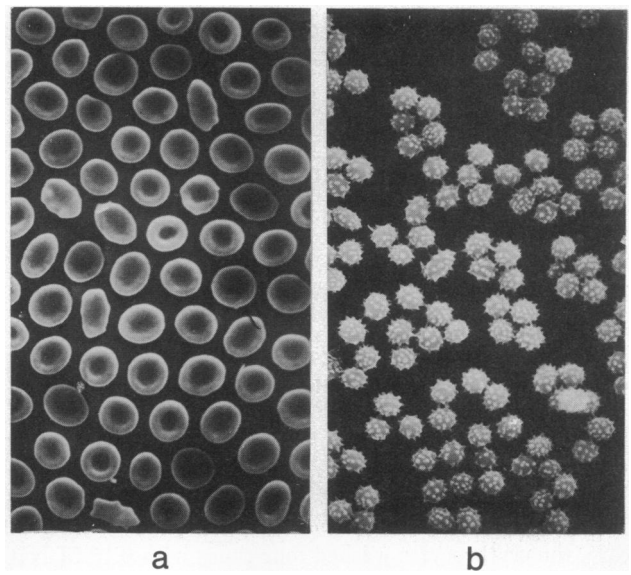

FIG. 1. Representative populations of control erythrocytes (a) and erythrocytes treated with 10^{-5} M 5NS (b), used for statistical evaluation. Magnification 750×.

about 0.84. Relative hemolysis values were calculated by dividing measured absorbance values by the absorbance of a reference sample incubated in test solution lacking nitroxide.

Electron spin resonance (ESR) spectra of the reaction mixtures were obtained at 5NS concentrations of 10^{-6} M to 5×10^{-5} M, with a Varian E3 ESR spectrometer.

RESULTS

Fig. 1 constitutes representative, low-magnification micrographs of untreated erythrocytes (Fig. 1a) and cells exposed to 10^{-5} M 5NS (Fig. 1b). Fig. 2 shows the details of the topological transformations induced by 5NS and correlates these with the osmotic stabilization–labilization produced by this reagent. Most of the control erythrocytes exhibit a biconcave morphology (Figs. 1a and 2a). 11% of the cells deviate from this appearance and display one to three knob-like protuberances, 1–2 μm in diameter, usually near the cell perimeter.

Exposure of the cells to low levels (10^{-10}–10^{-7} M) of 5NS increases the proportion of cells bearing knobs (Figs. 2b and c). Thus, evaluation of 847 control cells (seven randomly selected fields) yields 10.82% knob-bearing cells (SD ± 4.69%), whereas a count of 936 cells exposed to 10^{-10} M 5NS (seven randomly selected fields) gives 15.23% knob-bearing cells (SD ± 3.76%). A t test of the significance between the means of the samples indicates to a confidence limit of 95%, that 10^{-10} M 5NS, produces focal erythrocyte surface perturbations. Rising nitroxide concentrations increase both the proportion of anomalous cells and the number of surface protrusions per cell.

Between 10^{-7} and 10^{-6} M 5NS, more than 99.0% of the biconcave cells disappear. The cells become discoid and develop multiple surface protrusions. At 10^{-6} M the protuberances are still in the form of knobs and range between 2 and 5 per cell surface visualized or 4–13 per cell (Fig. 2d). Edge-on views of cells exposed to 1×10^{-6}–2.5×10^{-6} M 5NS indicate that, at these concentrations the cells are essentially disc-shaped with the surface protrusions extending from the two flat surfaces.

Between 1×10^{-6} M and 5×10^{-6} M, the surface protrusions increase to 28.2 ± 5.3 (SD) per cell and many cells develop a spherical symmetry (Fig. 2e). At 5×10^{-6} M most of the surface processes are irregularly conical with a base diameter of about 0.5 μm, a total height of about 1.7 μm of which about 0.5–1.0 μm corresponds to a cylindrical tip of about 0.2 μm in diameter*.

Between 5×10^{-6} M and 10^{-5} M, the number of projections per cells increase from 28 to 45 ($P < 0.01$) and > 99.9% of the cells assume a typical echinocyte appearance (10) with about 55 processes per cell. Between 10^{-5} M 5NS and 7.5×10^{-5} M, concentrations in which the cells lyse, another surface transformation occurs (Fig. 2f–h). Thus, at 2.5×10^{-5} M (Fig. 2g), the cell become spherical and bears 20 to 120 small processes. When the number of projections is large, the projections are very regularly distributed. The protrusions are approximately 1 μm in diameter and approximately 1 μm high. The area between processes is smooth at this level of resolution. Some cells appear virtually bald. At 5×10^{-5} M 5NS (Fig. 2h), we find 17 to 130 processes per intact cell and also many ruptured cells. Lysis is complete by 10^{-4} M.

The morphologic changes induced by up to 5×10^{-5} M 5NS are fully reversible within minutes. This can be shown by addition of normal cells, washing the echinocytes, or addition of fat-free serum albumin. Possible ATP depletion of the cells can thus be excluded as a mechanism. The phenomenon is not influenced by the presence of 10^{-2} M *N*-ethylmaleimide, which blocks all membrane SH groups including those of intracellular glutathione.

The bottom panel of Fig. 2 correlates the morphologic transformations induced by 5NS with its effect on erythrocyte osmotic stability (7, 8). The method lacks the sensitivity to detect osmotic stabilization at 5NS concentrations below 10^{-8} M. Above 10^{-8} M, osmotic stabilization increases in parallel with the echinocyte transformation. Maximal stabilization coincides precisely with maximal echinocyte formation. Furthermore, the destabilization phase corresponds exactly with sphere transformation. Cell lysis occurs above 5×10^{-5} M in both systems.

5NS and 16NS maximally stabilize erythrocyte membranes at different concentrations, i.e., 6×10^{-6} M and 3.5×10^{-5} M, respectively (Fig. 3), although their only structural difference is the position of the nitroxide group. This lies near the carboxyl in the first compound and near the methyl terminal in the second. We also find that 16NS is about four times more soluble in aqueous media as 5NS, and we, therefore, suspect that the two compounds are not distributed identically between the bulk aqueous phase and the erythrocyte membranes. It is possible, therefore, that the two nitroxide stearates behave identically at equivalent concentrations in the membrane and that this is attained at a lower bulk concentration in the case of 5 NS. However, we cannot exclude the possibility that 5NS is the more potent perturbant. Stearic acid up to a concentration of 10^{-5} M does not stabilize nor labilize erythrocytes under our conditions. ASL and SAMSL yield stabilization-labilization sequences similar to the stearate

* ESR spectra of 5×10^{-6} M solutions of 5NS in buffered saline that contain 3.3×10^{6} erythrocytes per ml show a maximum hyperfine splitting of 55 gauss and the bandwidth of the central line is 5.6 gauss; the latter values are typical for erythrocyte membranes.

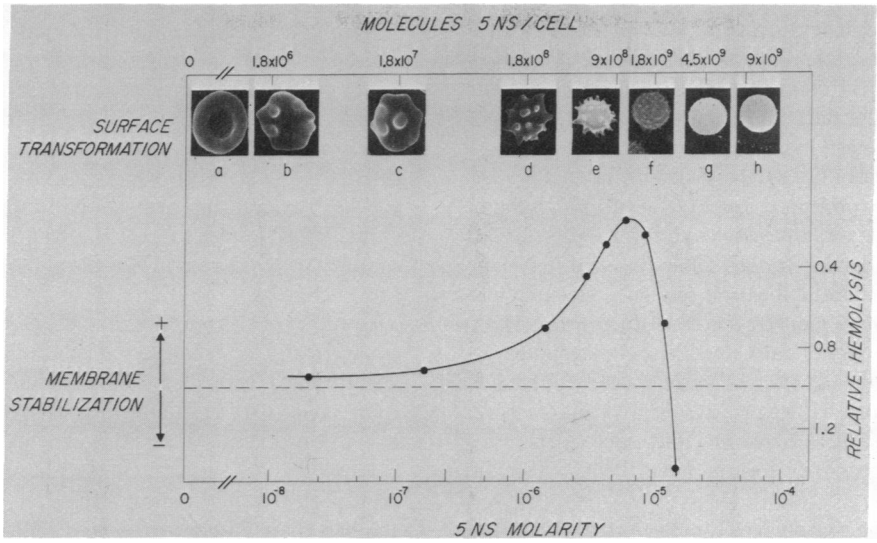

FIG. 2. Correlation between surface transformation and osmotic fragility of human erythrocytes as a function of 5NS concentration. Details are given in text. Magnification throughout 1050×.

nitroxides (Fig. 4), but maximum stabilization occurs near 3 × 10^{-5} M. SAMSL does not confer the same degree of osmotic protection as the other compounds.

The cholesterol analogue, ASL, causes the same sequence of topologic alterations as described for the stearate derivatives. However, as expected from Fig. 4, the structural changes occur at higher bulk concentrations. The dimensions and distributions of the surface projections resemble those produced by 5NS (Fig. 2) but the progression is less uniform from cell to cell.

Hemoglobin-free erythrocyte ghosts show no change in surface topology after exposure to nitroxides under the same conditions as those used for obtaining the data shown in Figs. 1–4. They appear as collapsed sacs without knobs or other surface protuberances.

DISCUSSION

Lipoidal spin labels have been used to characterize the perturbations induced in isolated erythrocyte ghosts by diverse, extraneous small molecules (11). Here we examine four such nitroxide lipid analogues to test whether they do not themselves function as membrane perturbants. The two stearate derivatives differ in the position of the nitroxide residues in the fatty acid chain; in the androstane and stearamide analogue, the nitroxide residues lie at the polar ends of the molecules. In isoosmotic buffers, low concentrations of all labels produce echinocytes; at high concentrations they cause cell lysis. In hypotonic buffers, low concentrations of all compounds tested reduce osmotic fragility. However, concentrations just slightly above the maximum stabilization level, produce full hemolysis. Under isotonic conditions the prelytic effects are reversible.

We observe morphologic changes over the range of 1.8 × 10^4 to 1.2 × 10^{10} molecules per cell and osmotic effects between 1.8 × 10^6 and 1.2 × 10^{10} molecules per cell. The stabilization-labilization sequence found under hypoosmotic conditions follow patterns typical for "nonspecific" hemolysins, e.g., numerous surfactants, diverse lipid soluble substances, lipophilic drugs, local and general anaesthetics (12–14). However, the concentrations for maximal stabilization and lysis place the four nitroxides among the more potent membrane perturbants.

The stabilization-labilization sequences seen between 1.8 × 10^6 and 1.8 × 10^{10} molecules per cell, correlate well with the progressive alteration of surface topology observed in isotonic media. In cells which are osmotically sphered, we cannot detect the focal membrane perturbations seen in isotonic media. However, we find an exact parallel between the stabilization conferred by the nitroxide upon osmotically stressed cells and the transformation to the echinocyte form, seen under isotonic conditions. Indeed the echinocyte transformation induced by the spin probes is exactly that described by Bessis (10). A similar parallel exists between the sphering-lysis reaction, seen under isotonic conditions at high perturbant levels, and the destabilization of the membranes of osmotically stressed cells. We therefore reason that the

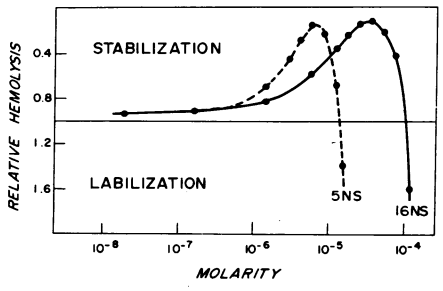

FIG. 3. Stabilization (relative hemolysis <1) and labilization (relative hemolysis >1) of human erythrocytes against osmotic lysis at various bulk concentrations of 5NS and 16NS.

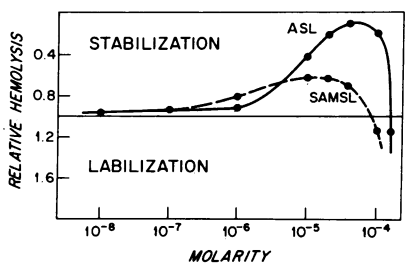

FIG. 4. Stabilization-labilization curves for ASL and SAMSL.

echinocytes and pre-echinocytic forms possess greater than normal osmotic stability, whereas the post-echinocytic stages exhibit impaired osmotic stability. This view is consistent with the recent studies of Sato and Fujii (15) on the effects of lysolecithin on erythrocyte membranes†.

The membrane perturbations observed with nitroxide analogues resemble those produced by diverse amphiphilic or lipophilic agents. However, the extensive information about the behavior of the nitroxide probes allows substantial clarification of the stabilization-labilization sequence. Seeman and associates (16, 17) have demonstrated that during the stabilization of spherical, osmotically swollen erythrocytes by various membrane active agents, the surface area can expand 5–7% before lysis occurs. However, our electron microscopic observations and those in (18), show that such surface expansion is not distributed uniformly over the surface, but occurs in focal regions.

We detect clear changes of surface topology at 10^{-10} M 5NS, i.e., 3×10^{-20} moles per cell or 2×10^4 molecules per cell. If we assume the cell surface to be a bilayer shell, partition all 5NS molecules into this shell, and distribute the probe molecules equally within the two bilayer leaflets, we obtain 10^4 molecules per bilayer. At low surface tensions such as exist at cell surfaces (< 2 dynes/cm) stearic acid occupies an area of 20 Å^2 per molecule. For 12-nitroxide stearate the value exceeds 130 Å^2 per molecule (4). We assume that 100 Å^2 per molecule is a reasonable approximation for 5NS. Then 10^4 molecules per cell bilayer would extent the cell surface by about 10^6 Å^2. With a cell surface area of 137×10^8 Å^2 (8), this corresponds to an undetectable factor of 0.07%.

However, at 2×10^4 molecules of 5NS per cell we observe only an increment of 4.5% in abnormal cells; this proportion increases to >99.9% by 10^9 molecules per cell. It is possible that the label binds equally to all cells even at 2×10^4 molecules per cell, but to estimate the maximum possible area expansion at the low 5NS level, let us assume that the probe has entered abnormal cells only. Distributed over the full cell surface area this gives an area expansion of 0.18%, which is also below detection limits.

How can one explain the increased proportion of cells showing *focal* protrusions at 2×10^4 molecules of 5NS per cell? We consider the following possibilities:

First, insertion of the nitroxide produces membrane expansions at "soft" sites quite unrelated to the probe location. Such a mechanism is possible but vague. Also one cannot address it in terms of established data.

Second, concentration of nitroxide molecules in certain surface domains causes membrane protrusions at these sites. However, can mere insertion of 5NS into defined bilayer domains produce the observed focal changes? To test this question we assume that all the added nitroxide binds only to altered cells and that they localize exclusively into circular bilayer domains, with restrained perimeters of radius 6×10^3 Å (the average values of the area subtended by the knobs at 2×10^4 molecules per cell) and areas of about 1×10^8 Å^2. Let us assume that the knob-base perimeters represents the limits of these domains. The average number of knobs per cell in the 4.5% abnormal cells is four, giving a total area of about 4×10^8 Å^2. With these assumptions the nitroxide molecules would contribute not more than 2×10^7 Å^2 (even though their local concentration, assuming a 75 Å membrane thickness, would approximate 10^{-3} M). Since the knobs are nearly hemispherical, i.e., their surface area is twice that of their bases, each protrusion represents an area increase of 2×10^8 Å^2. The limiting area contribution of 5NS is $^1/_{10}$ of this value. We therefore suspect that the area added by the probes cannot, by itself, account for the emergence of focal membrane protuberances.

In intact erythrocytes the osmotic pressure of hemoglobin is countered by ion transport mechanisms and by cohesive forces within the membrane. Independent studies (17) show that there is no K^+ leakage during the stabilization phase induced by various agents. This fact, as well as the rapid kinetics of the topologic changes (compare also ref. 10) weigh against ion transport as a mechanism. However, lipid nitroxides tend to fluidize their microenvironment. They would, therefore, not only expand the areas where they localize, but also weaken lateral cohesions within these regions. This would produce localized membrane protrusions. This might come about whether the nitroxides associate with lipids, proteins or both. The lack of membrane protrusions in treated hemoglobin-free ghosts, in contrast to the behavior of hemoglobin-containing ghosts, supports the proposed mechanism.

Our proposal is partially consistent with nuclear magnetic resonance studies of Metcalfe and associates (19, 20) showing that during stabilization sequence diverse membrane-active compounds partition into a hydrophobic phase. These data, as well as studies (11, 21) in which spin labels are used to monitor the membrane effects of other perturbants, indicate that membranes become increasingly fluid with rising bulk concentrations of perturbant. However, as shown by our electron microscopic data, the perturbations are not distributed throughout the membrane, but occur in limited domains. Moreover, our observations on erythrocyte ghosts demonstrate (22) that, at nitroxide levels equivalent to 3×10^8 molecules per cell (6×10^{-7} M) there is appreciable binding of spin label to membrane proteins.

The comparison of ASL and 5NS is informative. Both substances would insert a nitroxide residue at about the same depth in a hypothetical lipid bilayer. But the range and type of motion differ for the two probes. In ASL the nitroxide residue is rigidly fixed to the rest of the compact molecule. The principal motion of ASL is that of spinning about an axis perpendicular to the membrane surface. In contrast, the structure of 5NS will allow rotations about methylene groups and, importantly, flexing of the hydrocarbon chain. Also, cholesterol nitroxide analogues occupy lesser areas at air water interfaces than nitroxide stearates (4). The lesser perturbing efficiency of ASL thus follows its known properties.

Turning to the labilization phase (2×10^9 to 10^{10} molecules per cell), our electronmicroscopic data indicate an abrupt breakdown in the "domain" structure of the membrane. Furthermore, nuclear magnetic resonance studies (19, 23, 24) indicate that *membrane proteins* become irreversibly and drastically altered during this phase. We suggest that the hypothicated membrane domains involve membrane proteins interacting directly and/or via membrane lipids by apolar interactions; these forces become weakened when the concentrations of the active agents *in* the membrane reach a critical level.

† These authors find that at lysolecithin concentrations that give 96% cell lysis (about 10^{-4} M) the ratio of lysolecithin to total of other cell lipids is 0.036, as compared with 0.012 in control cells.

To sum, our data suggest that, (*a*) lipid nitroxide analogues may not associate with all the cells in a population, (*b*) the spin probes may not sample the whole area of a labeled cell. Our experiments further indicate that the spin labels perturb erythrocyte membranes and that this process can become irreversible.

Supported by Grants CA 13061 and CA 13252 from the U.S. Public Health Service, and Grant CB 43922 from the National Cancer Institute, Award PRA-78 from the American Cancer Society (D.F.H.W.) and Stiftung für Stipendien auf dem Gebiet der Chemie, Basel (V.G.B.).

1. Keith, A. D., Sharnoff, M. & Cohn, G. E. (1973) *Biochim. Biophys. Acta* **300**, 379–419.
2. Wallach, D. F. H. & Winzler, R. F. (1974) in *Evolving Strategies and Tactics in Membrane Research* (Springer-Verlag, New York), chap. 3.
3. Cadenhead, D. A. & Katti, S. S. (1971) *Biochim. Biophys. Acta* **241**, 709–712.
4. Tinoco, F., Ghosh, D. & Keith, A. D. (1972) *Biochim. Biophys. Acta* **274**, 279–285.
5. Mehlhorn, R., Snipes, W. & Keith, A. D. (1973) *Biophys. J.* **13**, 1223–1231.
6. Seeman, P. (1966) *Biochem. Pharmacol.* **15**, 1767–1774.
7. Seeman, P. (1968) in *Stoffwechsel und Membranpermeabilität von Erythrocyten und Thrombocyten*, eds. Deutsch, E., Gerlach, E. & Moser, K. (G. Thieme, Stuttgart), pp. 384–390.
8. Dodge, J. T., Mitchell, C. & Hanahan, D. F. (1963) *Arch. Biochem. Biophys.* **100**, 919–929.
9. Millonig, G. (1961) *J. Appl. Phys.* **32**, 1637.
10. Bessis, M. (1973) *Living Blood Cells and their Ultrastructure*, (Springer-Verlag, New York).
11. Hubbell, W. L., Metcalfe, J. C., Metcalfe, S. M. & McConnell, H. M. (1970) *Biochim. Biophys. Acta* **219**, 415–427.
12. Seeman, P. (1966) *Biochem. Pharmacol.* **15**, 1632–1637.
13. Seeman, P. & Weinstein, J. (1966) *Biochem. Pharmacol.* **15**, 1737–1752.
14. Seeman, P. (1966) *Biochem. Pharmacol.* **15**, 1753–1766.
15. Sato, T. & Fujii, T. (1974) *Chem. Pharm. Bull.* **22**, 152–156.
16. Seeman, P., Kwant, W. D. & Sauks, T. (1969) *Biochim. Biophys. Acta* **183**, 490–498.
17. Roth, S. & Seeman, P. (1972) *Biochim. Biophys. Acta* **255**, 190–198.
18. Fujii, T., Sato, T. & Nakanishi, K. (1973) *Physiol. Chem. Physics* **5**, 423–430.
19. Colley, C. M., Metcalfe, S. M., Turner, B., Burgen, A. S. V. & Metcalfe, J. C. (1971) *Biochim. Biophys. Acta* **233**, 720–729.
20. Metcalfe, J. C. (1971) in *The Dynamic Structure of Membranes*, eds. Wallach, D. F. H. & Fischer, H. (Springer-Verlag, Heidelberg) p. 202.
21. Hubbell, W. L. & McConnell, H. M. (1968) *Proc. Nat. Acad. Sci. USA* **61**, 12–16.
22. Wallach, D. F. H., Verma, S. P., Weidekamm, E. & Bieri, V. (1974) *Biochim. Biophys. Acta* **356**, 68–81.
23. Metcalfe, J. C., Seeman, P. & Burgen, A. S. V. (1968) *Mol. Pharmacol.* **4**, 87–95.
24. Metcalfe, J. C. & Burgen, A. S. V. (1968) *Nature* **220**, 587–588.